

High-Rate Underwater Acoustic MIMO Communication Using Adaptive Passive Time Reversal: Demonstrations in Shallow Water Channel

Yukihiro Kida Takuya Shimura* Kenjiro Okadome
Mitsuyasu Deguchi

Japan Agency for Marine-Earth Science and Technology, Yokosuka, Japan

ABSTRACT

In underwater acoustic channel, it is very difficult to achieve reliable or high-rate communication because of the narrow bandwidth, very large Doppler effect, and strong multipath interference, comparing with those in radio communication in air. To overcome these difficulties, time-reversal decision feedback equalizer (DFE) is a promising solution as a channel equalization, and in previous study, a long-range communication with single-input/multiple-output (SIMO) at 600 km in deep water was achieved at the spectral efficiency of 3.7 bps/Hz using passive time-reversal DFE. In this study, adaptive passive time-reversal (APTR) DFE is applied for spatial division multiplexing (SDM) based multiple-input/multiple-output (MIMO) communication and verified in shallow water experiments. The experiments were conducted in water depth 200 m, at the range of 13.5 km, with spatial multiplexing up to 5 channels. As a result, the effective data rates of 30 kbps were achieved at 90 % of bit-error free packet rate. The spectral efficiencies were over 6.6 bps/Hz in these results. Thus, it is demonstrated that adaptive passive time-reversal is a very effective method to realize very high-rate MIMO communication in a multipath rich acoustic channel.

Keywords: *Time Reversal, Decision Feedback Equalizer, Single Carrier, MIMO, Underwater Acoustic Communication.*

1. BACKGROUND

As is very well known, the narrowband characteristic of underwater acoustic channels is a factor that directly limits the data rate of underwater acoustic communication (UWAC), and it is necessary to improve the spectral efficiency in units of bps/Hz to achieve the high data rate communication system. In band-limited underwater acoustic environment, the MIMO communication technique is considered as one of the promising solutions for improving the spectral efficiency via the simultaneous signal transmissions from multiple transmitters. There have been many efforts suggested the various approach of the MIMO communication techniques in UWAC, including the approach for multi-carrier modulation schemes in the form of orthogonal frequency division multiplexing [1-3], single carrier modulation combined with multichannel decision feedback equalizer [4], turbo equalization [5] and etc. However, especially in long range communication, the improvement of the spectral efficiency has been relatively limited compared with the MIMO communication system in air radio wave communications.

Passive time-reversal (PTR) communication techniques, which is the receiver side processing mathematically equals to the channel matched filter using a prior knowledge of channel response, combined with a single channel DFE have been widely applied for multipath rich long range UWAC [6-9]. Furthermore, a time-reversal technique called adaptive passive time reversal (APTR) has been applied to the SDM MIMO communication in UWAC, and literatures have shown that the APTR-DFE approach can be considered as an attractive solution in multipath-rich long-range environment [10-13]. Specifically, the APTR-DFE approach was firstly applied to a 20 km long range UWAC MIMO utilizing the bandwidth from 3 to 4 kHz in shallow water channel [10]. In deep water, very low frequency sources of 500 Hz were utilized for MIMO communication,

*Corresponding author: Acoustics237@jamstec.go.jp

Copyright: ©2023 First author et al. This is an open-access article distributed under the terms of the Creative Commons Attribution 3.0 Unported License, which permits unrestricted use, distribution, and reproduction in any medium, provided the original author and source are credited.

and they successfully demodulated quadrature phase shift keying (QPSK) signals up to 6 transmission channels [11]. While there have been several promising research outcomes regarding APTR-DFE, there are also limitations such as the use of low-frequency narrowband signals resulting in a slow data rate, as well as a scarcity of test cases in real-ocean environments and reports limited to a small number of research groups.

In this study, a sea trial of long-range MIMO UWAC is reported, to propose and experimentally verify a high data rate MIMO communication system using APTR with relatively wide 4-8.5 kHz frequency bandwidth. In our recent related research [13], we have reported SDM-MIMO communication with up to four channels, achieving a 24 kbps link in the communication distance of 12.5 km at a middle water depth of 750 m with moderate uncoded BER quality. However, our current focus is on pursuing further improvements in data rate and the applicability in relatively shallow sea channels. We evaluate the experimental data focusing on the effective data rate and error rate while changing signal parameters, and discuss the effectiveness in a 200 m depth real sea environment.

2. MIMO RECEIVER ALGORITHMS

The receiver algorithms for MIMO communication system are presented in this section. The key structure for receiver signal processing is summarized in Fig. 1.

2.1 Signaling and channel estimation

First, the communication signaling frame to be processed by the receiver algorithms is described in this subsection. The signaling frame designed for the experiment is shown in Fig. 2.

The channel probing signal is transmitted prior to the information signal for the estimation of the channel response among the transmitters and receivers. Linear frequency modulation signals generated by the Zadoff-Chu sequence [14-15] are utilized for the channel probing. In the Zadoff-Chu sequence, by shifting the starting phase, the time peak position of the cross-correlation function can be adjusted. This allows simultaneous measurement of channel responses during multi-channel transmission, while also achieving savings in guard time and maintaining correlation gain. The channel estimation is performed by the matched filtering processing with the replica signals. The channel probing signals are transmitted simultaneously from transmitters, and the received interfered signals are distinguished into each transmission by using the orthogonality of the Zadoff-Chu sequence. The estimated

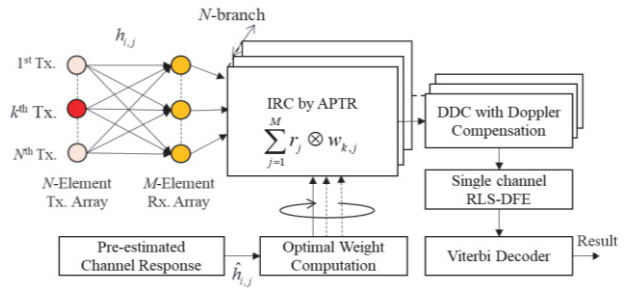


Figure 1 APTR receiver structure for MIMO communication.

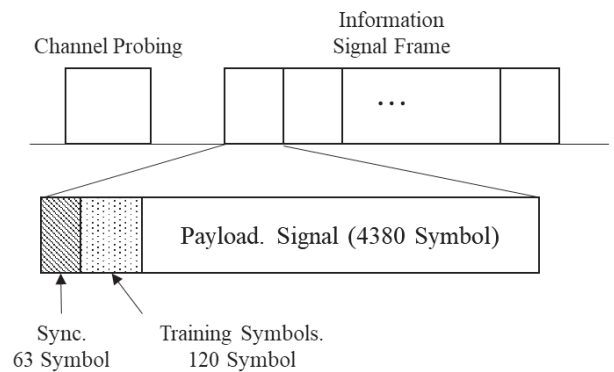


Figure 2 Signaling Frame

Table 1 Key Signaling Parameters

Parameter	Value
Number of Transmission Channels	Up to 5 Ch.
Carrier Frequency	6.25 kHz
Symbol Rate	4.5 kHz
Roll-Off Factor	0.15
Modulation	SC-QPSK
Slot Size	4563 symbols
Data Symbols in a Slot	4380 symbols
Channel Probing	1.2 s
Information Signal Length	1 - 16.2s
Effective Rate (coded)	3.3 - 33.5 kbps

channel responses are utilized for the computation of the weight function for the interference rejection combining in APTR method. It should be noted that the channel response estimated using the channel probing signal may not necessarily match the channel response in the subsequently received communication signals due to the temporal variation of the channel.

The information signal frames are composed of sequential form of subframes including the synchronization code,

training symbols for filter tap estimation of the equalizer, and the payload which are modulated by single carrier modulation scheme. The Zadoff-Chu sequence of 63 symbols is utilized for the synchronization code. The training symbols are generated from the pseudo-random bit sequence modulated by phase shift keying. The symbols of payload signals are generated from the convolutionally coded bit sequences with the coding rate of 5/6 modulated by the phase-shift keying. Key parameters for signaling frame in the experiment are summarized in Tab. 1.

Accounting for all the overheads due to the channel probing duration, training symbols, synchronization codes for signal slot detection, and the channel coding, the overall spectral efficiency in terms of bps/Hz of the MIMO communication system can be computed. The effective data rate of the system is changed by changing the number of transmission channels and the ratio of the length of information signal frame to the signaling overhead. The number of simultaneously transmitted channels was varied from 1 to 5 channels. The length of the transmitted signal was varied by changing the length of the information signal frame, which was continuously transmitted, from 1 to 16 frames, resulting in a variation of approximately 1 to 16.2 seconds.

2.2 Adaptive passive time-reversal

We consider spatial division multiplexing MIMO communication from N transmitter channels to M elements receiver array. The system model for received signal at j^{th} elements of receiver array $r_j(t)$ can be expressed as follows:

$$r_j(t) = \sum_{i=1}^N h_{i,j}(t) * s_i(t) + z_j(t), \quad (1)$$

where $h_{i,j}(t)$ is channel response between i^{th} transmitter and j^{th} receiver, $s_i(t)$ is the transmitted signal from i^{th} transmitter, $z_j(t)$ is the background noise, and $*$ denotes the convolution.

In APTR receiver, the estimated channel responses for matched filtering process in PTR are optimized to minimize the crosstalk among multiple transmitters. The optimal weight function for k^{th} transmission channel in frequency domain $W_{k,j}(f)$ can be obtained from spectrum of the estimated channel response $H_{i,j}(f)$ by solving following optimization problem [16]:

$$\min_{\mathbf{w}} : \mathbf{w}_k^H \mathbf{R} \mathbf{w}_k, \text{ s.t. : } \mathbf{w}_k^H \mathbf{d}_k = 1, \quad (2)$$

where, overscript of $[]^H$ is conjugate transpose. The vector form of optimal weight \mathbf{w} , estimated channel

response \mathbf{d} , and the cross-spectral density matrix of estimated channel response \mathbf{R} is defined as follows:

$$\begin{aligned} \mathbf{R} &= \sum_{i=1}^N \mathbf{d}_i \mathbf{d}_i^H + \sigma^2 \mathbf{I} \\ \mathbf{d}_i &= [H_{i,1}(f) \dots H_{i,M}(f)]^T \\ \mathbf{w}_k &= [W_{k,1}(f) \dots W_{k,M}(f)]^T, \end{aligned} \quad (3)$$

where, $[]^T$ indicates the transpose, $\sigma^2 \mathbf{I}$ is the small diagonal load on the cross-spectral density matrix. The optimization problem Eqn. (3) can be solved by using Lagrange multiplier and the optimal weight function can be computed as:

$$\mathbf{w}_k = (\mathbf{d}_k^H \mathbf{R}^{-1} \mathbf{d}_k)^{-1} \mathbf{R}^{-1} \mathbf{d}_k. \quad (4)$$

After taking the inverse Fourier transform, the weight function in time domain $w_{k,j}(t)$ can be obtained. In APTR receiver, the received signal is cross-correlated with the optimal weight function $w_{k,j}(t)$ and summed over the receiver elements, then the signal from each transmitter $u'_i(t)$ can be decomposed as:

$$u'_i(t) = \sum_{j=1}^M r_j(t) \otimes w_{k,j}(t), \quad (5)$$

where \otimes is the cross-correlation operator. From expressions Eqn. (4) and (5), it can be interpreted that APTR is equivalent to the minimum variance distortionless response (MVDR) beamformer for wideband signals to suppress co-channel interference (CCI) using the prior knowledge of the channel response. As shown in Fig. 1, the APTR process is applied first to the received signals in passband, and the signals are decomposed into each transmission stream.

2.3 Doppler Compensation and Equalization

As shown in Fig. 1, after APTR process, synchronization detection of the signal frame was performed in the passband region using correlation processing with a replica signal. Coarse correction of Doppler shift was performed during baseband symbol conversion using the results of this synchronization detection. The received signal symbols were equalized using a DFE with a digital phase locked loop (DPLL), feedforward filter, and feedback filter. The filter coefficients of the DFE were updated using a recursive least squares algorithm.

From the soft output results of the decision feedback equalizer, log-likelihood ratios (LLR) were calculated and bit decoding was performed using a soft decision Viterbi

decoder. The LLR is calculated by an approximate LLR method quantized with 8 bits.

3. EXPERIMENTAL RESULT

A long range underwater acoustic MIMO communication experiment was carried out in an area of 200 m depth above the continental shelf on the Pacific coast of Japan in July, 2021. A vertical transmitter array which consists of 5 projectors and a receiver array which consists of 24 hydrophones are deployed to collect experimental data. The distance between the transmitter array and the receiver array was about 13.5 km. The projectors of the transmitter array were equally spaced with a spacing of approximately 6 m. Each projector transmitted the communication signal at the acoustic level of about 182 dB.re.μPa@1m. The aperture of the receiver array was about 24 m. The top elements of both arrays were moored at a depth of approximately 140 m. The bathymetric profile between transmitter and receiver is gentle terrain and can be regarded as approximately equal depth.

An example of the temporal variation in the delay-power profile of the estimated channel response between the transmitters and receivers at the top of the array is shown in Fig. 3. Sparse delay spread of about 150 ms was observed, and large amplitude arrivals were observed within a range of about 50 ms from the initial arrival wave. Amplitude fluctuations were observed in later multipath waves, but the time variations of the earlier arrivals with large amplitudes were relatively small.

Figure 4 shows the temporal coherence function of the channel response [17] estimated from successive transmissions of chirp signal records from the deepest element of the transmitter array. On average, the temporal coherence value remains relatively high, around 0.9, for approximately 10 seconds, indicating a relatively stable channel environment. However, as time progresses, there are instances where the temporal coherence significantly decreases depending on the time period. Overall, the characteristic to maintain a high temporal coherence value for around 10 seconds suggests that the APTR approach for array signal processing can be highly effective.

Figure 5 shows the cumulative distribution function of the uncoded bit error rate (BER) when the number of transmit channels was set to 3-5 and the signal duration was set to 6.1 and 12.2 seconds. Practical BER can be achieved for most of the data through signal equalization. However, as the number of transmit channels and information signal lengths are increased for improving data rate, there is a

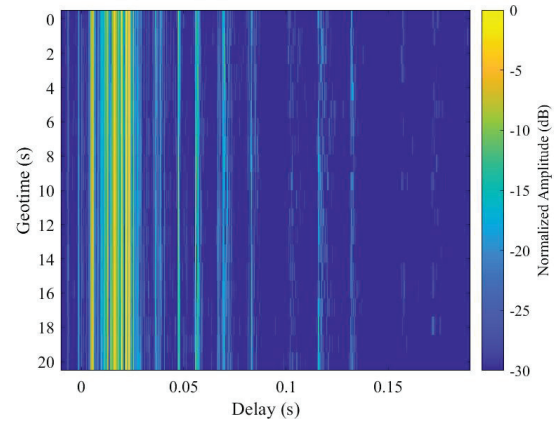


Figure 3. An example of channel delay-power profile.

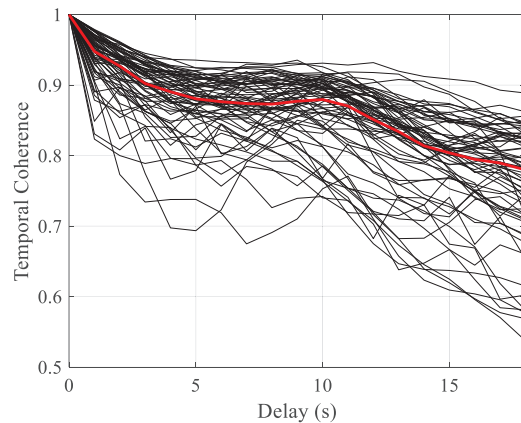


Figure 4. Temporal coherence function of estimated channel response from deepest transmit channel. The Bold line represents the mean value throughout the experiment.

tendency for error rate to increase. When the information signal length was set to 12.1 seconds with 3 or 4 transmit channels, the error rate distribution was similar to that of the case with 4 or 5 transmit channels and a communication signal duration of 6.1 seconds, respectively. Given that the per-channel uncoded transmission rates are 6.76 and 6.97 kbps for signal lengths of 6.1 and 12.2 seconds, respectively, it is considered that increasing the number of transmission channels is more advantageous for improving data rate.

When optimizing the system with a focus on achieving a low BER, it should be noted that using fewer transmission channels and shorter signal lengths can be advantageous. The optimal solution varies depending on the acceptable BER design criteria. To illustrate this relationship more clearly, we illustrated Figure 6, which shows the hierarchical distribution of uncoded BER for different numbers of transmission channels and signal lengths. The x-axis represents 16 patterns of signal lengths (1, 2, ..., 16.2 s), and the bar graphs group the hierarchical distributions for each number of transmission channels. Within the same number of transmission channels, the bar graphs from left to right represent increasing signal lengths. The hierarchical distribution is divided into six levels, ranging from $[0, 10^{-5}]$ to $[0.1, 1]$ with a logarithmic scale of 10. From the results, it can be observed that as the number of transmission channels or the signal length increases, the BER performance deteriorates. Thus, there is a trade-off between improving communication data rate through increased signal length or transmission channels and BER performance. Additionally, Fig. 4 shows a slight time variation in the channel response, and when using pre-estimated channel response, there is a tendency for the processing performance to gradually degrade due to increasing mismatch between the estimation and processing time points over time. Therefore, it is important to consider the time variation of the channel response when designing optimal communication systems. The relationship between the time variation of the channel response and the communication system design in this experiment has been more extensively discussed in our previous research [18]. Finally, we considered the optimal communication design in the context of pursuing communication speed in the experimental environment. Figure 7 shows the relationship between communication speed and error-free rate after soft Viterbi decoding in the MIMO experiment results. The improvement in data rate at the same number of transmission channels is due to an increase in the information signal length. By setting a certain acceptable error rate, it is possible to determine the optimal number of transmission channels and communication signal length from the perspective of achieving higher data rates using the relationships in Fig. 7. Here, let's assume that we evaluate the packet error-free rate at 90%, for example. For transmission channel numbers of 3, 4, and 5, the maximum data rate that achieve a 90% packet error-free rate are approximately 20.5, 26.0, and 30.1 kbps, respectively, confirming that communication speed was surely improved without compromising the stability of the communication channel in this environment.

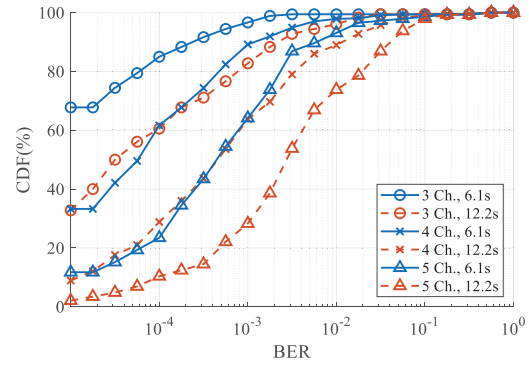


Figure 5 CDF of uncoded BER results.

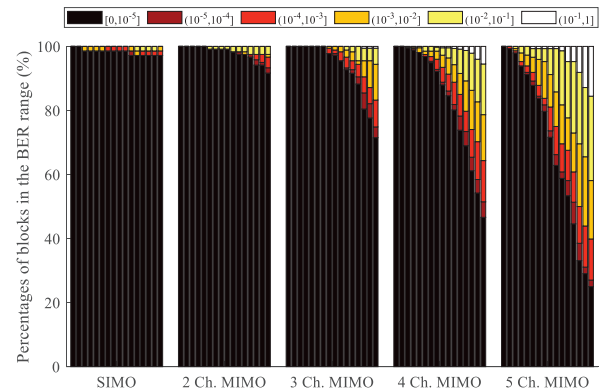


Figure 6 Hierarchical distribution of the uncoded BER for different number of transmission channels.

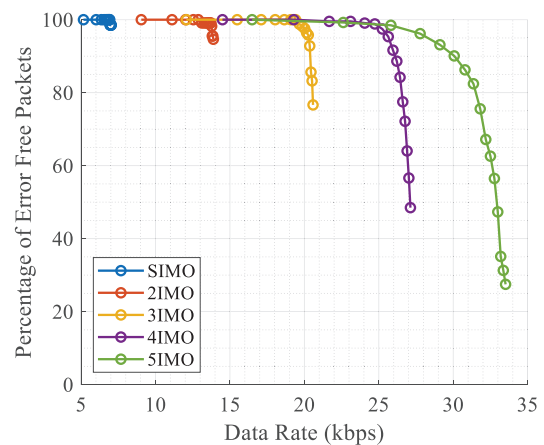


Figure 7 Data rate versus packet error-free rate in MIMO experiment results.

4. CONCLUSION

In this study, an APTR receiver structure for MIMO UWAC system was proposed, and applied to at-sea experiment data of long-range MIMO UWAC to investigate the effectiveness. As a result, it has been demonstrated that a data rate of 30.1 kbps can be achieved with a packet error free rate of 90% or higher at a distance of 13.5 km, using the optimal signaling.

Here, we conducted communication evaluations in an environment with relatively small temporal variation of the channel response. It is a concern that performance may degrade in environments with larger channel response variations. Therefore, further research on methods that consider compensation for time variation would be necessary. We have already conducted data acquisition in different marine environments showing much severe temporal variations, and we plan to report the analysis results in the future.

5. ACKNOWLEDGMENTS

This work was supported by the Innovative Science and Technology Initiative for Security program offered by the Acquisition, Technology & Logistics Agency (grant number: JPJ004596).

6. REFERENCES

- [1] B. Li, J. Huang, S. Zhou, K. Ball, M. Stojanovic, L. Freitag, P. Willet, "MIMO-OFDM for high-rate underwater acoustic communications," *IEEE J. Ocean. Eng.*, vol. 34, no. 4, pp. 634-644, 2009.
- [2] P. C. Carrascosa, and M. Stojanovic, "Adaptive channel estimation and data detection for underwater acoustic MIMO-OFDM systems," *IEEE J. Ocean. Eng.*, vol. 35, no. 3, pp.635-646, 2010.
- [3] Z. Li, D. Cuji, Y. Kida, M. Deguchi, T. Shimura, and M. Stojanovic, "Frequency offset estimation for high data rate acoustic MIMO-OFDM systems," *Proc. IEEE/MTS Oceans'23 Limerick*, 2023.
- [4] S. Roy, T. M. Duman, V. McDonald, and J. G. Proakis, "High-rate communication for underwater acoustic channels using multiple transmitters and space-time coding: receiver structures and experimental results," *IEEE J. Ocean. Eng.*, vol. 32, no. 3, pp. 663-688, 2007.
- [5] X. Qin, F. Qu and Y. R. Zheng, "Bayesian Iterative Channel Estimation and Turbo Equalization for Multiple-Input-Multiple-Output Underwater Acoustic Communications," *IEEE J. Ocean. Eng.*, vol. 46, no. 1, pp. 326-337, 2021.
- [6] H. C. Song, W. S. Hodgkiss, W. A. Kuperman, M. Stevenson, and T. Akal, "Improvement of time-reversal communications using adaptive channel equalizers," *IEEE J. Ocean. Eng.*, vol. 31, no. 2, pp. 487-496, 2006.
- [7] J. Gomes, A. Silva, and S. Jesus, "Adaptive spatial combining for passive time-reversed communications," *J. Acoust. Soc. Am.*, vol. 124, no. 2, pp. 1038-53, 2008.
- [8] T. Shimura et al., "Long-range time reversal communication in deep water: Experimental results," *J. Acoust. Soc. Am.*, vol. 132, pp. EL49-52, 2012.
- [9] H. C. Song, "An overview of underwater time-reversal communications," *IEEE J. Ocean. Eng.*, vol. 41, no. 3, pp. 644-655.
- [10] H. C. Song, J. S. Kim, W. S. Hodgkiss, and H. H. Joo, "Crosstalk mitigation using adaptive time reversal," *J. Acoust. Soc. Am.*, vol. 127, no. 2, EL19-22, 2010.
- [11] T. Shimura, Y. Kida, M. Deguchi, Y. Watanabe, and H. Ochi, "Experimental study on multiple-input/multiple-output communication with time reversal in deep ocean," *Jpn. J. Appl. Phys.* vol. 56, 07JG03, 2017.
- [12] D. Kim, H. Park, J. Kim, J. Y. Hahn and J. S. Park, "MIMO communication based on adaptive passive time reversal in deep water," 11th Int. Conf. on Ubiquitous and Future Networks (ICUFN), 2019, pp. 49-51.
- [13] Y. Kida, M. Deguchi, T. Shimura, "Experimental demonstration on long-range time-reversal multiple-input/multiple-output underwater acoustic communication over tens of kbps in 12.5 km range," *Jpn. J. Appl. Phys.*, vol. 62, SG1057, 2022.
- [14] R. L. Frank and S. A. Zadoff, "Phase shift pulse codes with good periodic correlation properties", *IRE Trans. Inform. Theory*, vol. IT-8, pp. 381-382, 1962.
- [15] D. Chu, "Polyphase codes with good periodic correlation properties," *IEEE Trans. Info. Theory*, vol. 18, no. 4, pp. 531-532, 1972.
- [16] Kim et al., "Adaptive Time Reversal Mirror," *J. Acoust. Soc. Am.*, vol. 109, pp. 1817-1825, 2001.



- [17] T. C. Yang, “Temporal coherence of sound transmissions in deep water revisited,” *J. Acoust. Soc. Am.*, vol. 124, no. 1, pp. 113-127, 2008.
- [18] Y. Kida, M. Deguchi and T. Shimura, “Experimental demonstration of spatial division multiplexing multiple-input/multiple-output underwater acoustic communication using a time-reversal method at the depth of the continental shelf: a consideration of optimization of signal length and number of transmission channels,” *Jpn. J. Appl. Phys.*, vol. 62, SJ1049, 2023.

